RSC Advances

ROYAL SOCIETY OF CHEMISTRY

www.rsc.org/advances

Synthesis of Highly Fluorescence Nitrogen Doped Carbon Quantum Dots Bioimaging Probe, Their In vivo Clearance and Printing Applications

Nargish Parvin[a,c] *and Tapas K. Mandal*[b,c]*

[a]Key Laboratory of Biochemical Engineering, Institute of Process Engineering, Chinese Academy of Sciences, No. 1, Bei Erjie, Zhongguancun, Beijing 100190, P. R. China.

[b]Institute of Chemistry, Chinese Academy of Sciences, Bei Yi Jie 2, Zhongguancun, Beijing 100190, China.

[c]Department of Biotechnology, Indian Institute of Technology, Roorkee, Uttarakhand 247667, India

Abstract:

Highly fluorescence, broad range pH and ionic stable N-doped carbon quantum dots (N-CQDs) were successfully synthesized and up to bottom characterized their chemical structure and fluorescence mechanisms. Mono-dispersed N-CQDs average sized 4.5 nm in diameter were achieved in a quantum yield (QY) of 74.16%. These N-CQDs showed great potential in biomedical and optical imaging applications in vivo and in vitro both. Biodistribution, retention, toxicity, and pharmacokinetics profiles are mandatory in their potential clinical applications. Here, the biodistribution, clearance, and toxicity of our invariable N-CQDs species were systematically investigated over a relatively 7 days in mice. Most of the N-CQDs were cleared at 6 days of post injection without any accumulation in any vital organ and tissues. Also the high fluorescence N-CQDs were demonstrated to be effective as printing inks for multicolor patterns. This study suggests that N-CQDs may be an attractive alternative to metal quantum dots for secure biomedical and other industrial applications.

Keywords: Nitrogen doped-Carbon quantum dots, bioimaging, bio distribution, clearance, multi color painting

Introduction

Recently nanomaterials are very interesting research tools for bioimaging, clinical diagnosis, bionic device and tissue engineering.[1-7] Semiconductor quantum dots (QDs) exhibit several unique photoelectric properties, such as size and wavelength-dependent luminescence and low photo-bleaching [8-10], due to their strong quantum confinement effects. QDs-based imaging integrates these properties to improve fluorescence imaging with the merits including real-time, accurate, and *in vivo* observations with high sensitivity, rapid responses, low costs, and no radiation. Other hand, researchers revealed the using of metal-based QDs (M-QDs) are involved with long-term toxicity and effected environment with heavy metals [11,12] The obtaining of M-QDs is a complex procedure and their storage also difficult without aggregation and chemical changes.[13] Normally Carbon QDs (CQDs) contained large amount of carbon with relatively less amount of oxygen, hydrogen and nitrogen causes it nontoxic and safest nano materials compare with heavy metals QDs.[14,15] It is favourable sized less than 10 nm of diameters[16], highly fluorescence and photostabilty,[17,18] and good storage observed.[17] In carbon dots the oxygen and hydrogen forms hydroxy and carboxyl groups, which facilitate the functionalization and improve the hydrophilicity.[16] Thus, CQDs are becoming a desirable alternative to M-QDs when taking their low toxicity, unique photophysical and chemical properties into considerations. Many complex synthetic methods, such as laser ablation, electrochemical oxidation, high temperature calcination, solvo thermal and microwave assisted pyrolysis, have been used to prepare CDs to date.[19] However, two issues that need to be addressed for the effective synthesis of cost-effective CDs still remain: the size non-uniformity and the time-consuming fabrication process.[20]

Doping CQDs with other non-metallic components is beneficial for adjusting the structure and composition and good fluorescence ink for printing.[21,22] N-doped CDs have been found to efficiently induce charge delocalization and enhance performance in bio-imaging and

catalysis with N atoms as dopants.[23] However, many scientific issues with C-QDs still awaits further investigation and large scale pharmaceutical applications are challenging in this field. Here we used agarose in combination with ethylenediamine passivated agents, to successfully prepare nitrogen doped Carbon quantum dots (N-CQDs) with enhanced fluorescence, high yield (74.16%), simple procedure, low cost, and high biocompatibility. And their imaging applications in an important model organism mice. In order to comprehensive clinical acceptance of these N-CQDs as a bioimaging agent, need to investigate toxicity, biodistribution, and clearance of nanoparticles in vivo Pharmacologic profiles,[24,25] routes of administration, biodistribution patterns, and dosage are all important considerations that are only beginning to be addressed in detail.[26-29]

So we demonstrated a multi-parametric in vivo study, clearance quantities, rates and toxicity determination of N-doped CQDs over short term (up to 7 days) time points. We observed that most of the N-doped CQDs were cleared before 7 days post injection in mice, without any major accumulation in any vital organ and tissues.

Experimental section

Synthesis of carbon nanoparticles

N-doped Carbon quantum dots (N-CQDs) were synthesized by hydrothermal treatment. Carbon source material agarose (2.5gm) and amine source 1ml ethylenediamine (EDA) added in 30 ml of water and mixed well in stirrer and then the mixture was transferred into an 80 ml teflon-lined stainless-steel autoclave and was heated at constant temperature of 200ºC for 1 to 6 hrs (2ºC/min) in separate sets. After the reaction is over, the autoclave was cooled down naturally. The product, which was brown-black and transparent, was subjected to dialysis in order to obtain the N-doped Carbon quantum dots (N-CQDs). The production yield was ca. 6-74% in different time conditions are listed in Table S2.

Fluorescent N-doped CQDs for printing. We used normal non fluorescence paper as a drawing paper. Aqueous N-doped CQDs ink was loaded into an empty ink pen (concentrations 0.01 mg mL^{-1} to 1mg mL^{-1}). The desired words or images were drawn onto a piece of "paper" by above ink pen. The fluorescence images were obtained under hand held UV lamp.

Cellular toxicity test. Breast cancer cell line (MCF-7) cells (1 X 10^4 cells/well) were cultured first for 24 h in an incubator (37°C, 5% CO_2) and for another 24 h after the culture medium was replaced with 100 µL of Dulbecco's modified Eagle's medium (DMEM) containing the N-doped CQDs at different doses (mg/ml). Then, 20 µL of 5 mg/mL MTT solution was added to every cell well. The cells were further incubated for 4 h, followed by removing the culture medium with MTT and then 100 µL of DMSO was added. The resulting mixture was shook for 10 min at room temperature. The optical density (OD) of the mixture was measured at 490 nm. The cell viability was estimated according to the following equation: $$Cell\ \ Viability\ \ (\%) = (\frac{OD_{Treated}}{OD_{Control}}) \times 100\%$$

(Where OD control was obtained in the absence of N-CQDs and OD treated obtained in the presence of N-CQDs).

Cellular imaging. The MCF-7 cells were cultured in DMEM supplemented with 10% fetal bovine serum and 1% penicillin. 0.1 mg mL^{-1} concentrated of N-doped CQDs solution were prepared in DI water. After the well dispersion, an aliquot (typically 100ul) of the suspension was added to culture plate, then incubated at 37°C in a 5% CO_2 incubator for 24 h. Prior to fixation of the cells on the slide for inspection with a fluorescence microscope, the excess N-doped CQDs were removed by washing 3 times with PBS. The bioimaging was taken at Zeiss inverted fluorescent Microscope (Carl Zeiss vert.A1 microscope, Carl Zeiss Micro imaging GmbH, 07740, Jena, Germany).

Organs imaging. The organs were harvested and cut into small pieces, fixed on glass slide and then directly subjected to microscopy study under fluorescence microscope.

Pharmacokinetics of N-doped CQDs. Eight weeks aged male mice (n=30) were housed in pairs in a standard 12 h light/dark cycle with food and water, ad libitum. The N-doped CQDs dose given was 5 mg/kg and intravenously injected into mice (n = 27). At 1hour, 4 hours, 12 hours and 1,2,3,4,5,6,7 day of post injection, the animals (n=3/day) were sacrificed. Blood samples were obtained via retro-orbital blood collection. The following organs and tissues including liver, spleen, kidney, lung and muscle were collected, weighed and dissected. The urine and faeces were continuously collected from mice housed in the metabolic cage. N-doped CQDs clearance was observed under fluorescence microscope. All animal experiments reported herein were carried out according to a protocol approved by IIT Roorkee ethical or animal care committee.

Quantum yields (QY) measurements.

Quinine sulphate (0.1M H_2SO_4 as solvent; QY=0.54) was chosen as standard. The QY of N-doped C-QDs (in water) was determined by slope method[1] by the reference of quinine sulphate: compared the integrated photoluminescence intensity and the absorbance value [several values (less than 0.1 at excitation wavelength) gave the curve] of the samples with that of the references.

Then used the equation: $\boldsymbol{\varphi x=\varphi st(Kx/Kst)(\eta x/\eta st)^2}$

Where φ is the QY, K is the slope determined by the curves and η is the refractive index. The subscript "*st*" refers to the standards and "*x*" refers to the unknown samples. For these aqueous solutions, $\eta x/\eta st=1$.

Statistical Analysis: All data presented in this study are the average ± SE of the experiments repeated at least three times. Paired Student's t-test was performed.

Materials characterization

High-resolution transmission electron microscope (HTEM) was carried out with JEM-2100F microscopes operating at 200 kV for characterizing the N-doped CQDs size and shape. AFM images were recorded in the tapping mode with a Nanoscope-III a scanning probe microscope from Digital Instruments under ambient conditions with Partial wafer of NanoSensors Pointprobes (type S3G3T6-8L224) where other settings were Integral Gain 0.5, Proportional Gain 0.7 and scanning rate 1Hz. Fluorescence spectroscopy was performed with a CARY Eclipse 5,5 fluorescence spectrophotometer and fluorescence spectra were measured using a 4 mL glass cuvette.

UV-vis absorption spectra were obtained using a CARY 50 Conc UV-vis spectrophotometer. IR spectra were taken on a Nicolet Nexus Aligent 1100 series FT-IR spectrophotometer. The fluorescent images were taken at fluorescence microscopy (Carl Zeiss vert.A1 microscope, Carl Zeiss Micro imaging GmbH, 07740, Jena, Germany). Using different band pass filtered 461nm, 560nm and 633 nm excitations and 5X,10X, 20PX Objectives. X-ray Photoelectron Spectroscopy (XPS) was investigated by using ESCALAB 250 spectrometer with a mono X-Ray source Al Kα excitation (1486.6 eV).

Results and discussion

The synthetic procedure is illustrated in Figure 1a. The reaction was conducted by first condensing agarose and ethylenediamine, whereupon they formed polymer-like carbon quantum dots (CQDs), which were then carbonized to form the CQDs. The morphology and particle size of CQDs were examined by TEM and AFM as shown in Figure 1b and 1c reveals that the CQDs are uniform and regularly spherical in shape with an average diameter of about 4.5 nm without aggregation. The corresponding particle size measured (Figure 1d) indicates that CQDs have a relatively narrow size distribution between 2 and 6 nm. The inset

in Figure 1b is a typical HRTEM image of CQDs shows the lattice spacing of 0.19 nm which corresponds to the [102] facet of graphitic carbon.[30]

XPS measurements were performed to identify the effective incorporation of nitrogen and surface functional groups of CQDs. From a survey scan of the XPS spectrum in Figure 1e three distinct peaks centred at 285.7 eV, 399.05 eV, and 532.1 eV can be observed, corresponding to C1s, N1s , and O1s respectively. Where the particle composed of carbon (C1s-51.73)%, nitrogen (N1s-12.79%) and oxygen (O1s-35.8%) (see in supporting information Table-S1).

In detail, the C1s spectrum (Figure 1f) displays three distinct peaks at 284.5 eV, 285.8 eV, and 287.6 eV, which are attributed to C–C, C–N, C O, respectively.[31,32] The N1s spectrum has two typical peaks at 399.2 (pyridinic Ns),[32] and 401.0 eV (pyrrolic Ns). [33] Figure 1g indicating that nitrogen is present in a π-π conjugated system where two p-electrons are present in the system of as-prepared CQDs.[23,] Its illustrating that the CQDs were successfully doped with nitrogen atoms. Figure 1h revealed that the O1s peak can be resolved into two components centered at 530.8 and 532.1 eV, representing the presence of the C=O and C-OH/-C-OC groups.[34,35] The XPS results indicate that the surface of the as-synthesized CQDs is functionalized by multiple oxygen and nitrogen-containing groups by the reaction between sucrose and ethylenediamine. Figure 2a shows the UV/Vis spectra, the peak was focused on 272 nm in an aqueous solution of N-doped CQDs (N-CQDs) where the fluorescence spectra of N-doped CQDs have optimal excitation and emission wavelengths at 390 nm and 474.54 nm respectively. Figure 2a inset represents the aqueous N-doped CQDs in a 4 ml cuvette under a white and UV lamp. Excitation-dependent fluorescence behavior was observed, which is common in fluorescent carbon materials in Figure 2b.[36-40] This behavior is contributed to the surface state affecting the band gap of N-doped CQDs. The surface state is analogous to a molecular state whereas the size effect is a result of quantum dimensions, both

of which contribute to the complexity of the excited states of N-doped CQDs.[41] Supporting Information Figure S1a exhibits the multicolour fluorescence images of N-doped CQDs under microscopy and fortunately we applied this excitation-dependent fluorescence character to acquire multi-color imaging of cancer cells (see Supporting Information Figure S1b).

Moreover, the surface groups were also investigated by FTIR analysis of N-doped CQDs. The FTIR spectrum in Figure 2c shows the characteristic absorption bands at 3403 cm^{-1} corresponding to the stretching vibrations of O–H and N–H.[42] The absorption bands at 1639 cm^{-1} and 1496 cm^{-1} are due to the C–O stretching vibrations and C–N stretching vibrations, respectively. The existence of carboxylic groups can be clearly proven by the peak at 2087 cm^{-1} corresponding to C O and the peak at 1042 cm^{-1} attributed to C–O, suggesting the partial oxidation of CD surfaces.[43] Furthermore, the band centered at 1395 cm^{-1} is assigned to the asymmetric stretching vibrations of the C–O–C bond.[44] It can be concluded from the results of XPS and FTIR analysis that the hydrothermal degradation of sucrose in the presence of EDA offered the as-synthesized N-doped CQDs with hydrophilic groups such as –COOH and –OH, which are beneficial for the improvement of aqueous solubility of N-doped CQDs for potential applications in biochemical uses, drug delivery and detection.

The XRD patterns of the N-doped CQDs (Figure 2d) also displayed a broad (002) peak centered at 24.20°, the corresponding interlayer spacing 0.42 nm, which is also attributed to highly disordered carbon atoms.[45]

Furthermore the fluorescence stability of N-doped CQDs to the effects of the ionic strength and pH of the solutions were investigated. There was no change in fluorescence intensity or peak characteristics at different ionic strengths (Supporting Information Figure S2), which is significant because it is necessary for N-doped CQDs to be used in the presence of physical salt concentrations in practical applications. Another interesting phenomenon is the pH-

dependent fluorescence intensity behavior (Supporting Information Figure S3). Fluorescence intensities decreased in a solution of high pH 14 or low pH 1, but remain constant in a solution of pH 2–13. This result may be a consequence of the chemical structure of N-doped CQDs, which have graphite lattices. The emission control of the surface state/molecule state was not affected by surrounding factors, such as solvent pH. At a pH that was too low/high, molecular groups are strongly affected.[39,46] So in our case It was found that redispersion of dry sample in water and other solvent without any aggregation, has great significance in preservation and transportation.

The time conditioning synthetic method can also be used to prepare different N-doped C-QDs (Supporting Information Table S2). Over these experiments, we found time is very important for the formation of high QY N-doped CQDs. 6 hours reaction produced QY 74% where 1hr 6% only (using quinine sulphate as a reference) (Supporting Information Figure S4).This is the best quantum yield performance according to our best knowledge (see Supporting Information Table S3). Supporting Information Figure S5 and S6 represents the comparative studies of excitation depended fluorescence spectra and open eye fluorescence intensity under white and hand held UV lamp respectively.

To make use of the high QY, the N-doped C-QDs were employed as ink for printing patterns on normal non fluorescing paper. Colourless aqueous solutions of N-doped C-QDs were loaded in ink pens. Used N-doped C-QDs concentration was 0.01mg mL^{-1} to 1mg mL^{-1} and gave strong enough fluorescence under a hand-held UV lamp. Fluorescing images and words were distinctly visible (Figure 3a-g). The fluorescence intensity was increased with the increasing concentration of N-doped CQDs used as printing ink. By using this property multicolour printing images were obtained (Figure 3d,e,f). Moreover, the printed patterns retained their stability after 1.6 years in a laboratory ambient environment, which is beneficial for practical applications (Figure 3g). An MTT assay showed that the N-doped

CQDs possess low cytotoxicity, and thus could act as an excellent bioimaging agent (See Supporting Information Figure S7). Human breast cancer cell MCF-7 after incubating with N-doped CQDs in a culture solution, the fluorescence in the cells sustained a high intensity, and the excitation-dependent fluorescence resulted in multicolour imaging under different excitation wavelengths (See Supporting Information Figure S1b).

High stability of N-doped CQDs in body fluid is crucial for their further in vivo applications. In Figure 4a-c shows the pre injection and post injections of whole body bio imaging of mice. After 12 hours of post injection it was given strong fluorescence intensity whole over the body (Figure 4b) but after 24 hours of post injection the body fluorescence intensity was still little remained (Figure 4c). This data clearly suggest that as-prepared N-doped CQDs were stable in the body fluid. After one hour of post injection, highly blood vessel oriented organs and tissue imaging studied under fluorescence microscopy. Results show the multicolour imaging under different excitation wavelengths (Figure 4d). It proved that our N-doped CQDs easily crossed the organ epithelial layer by Nano leaking process.[47-49] This fantastic feature also facilitates our in vivo biodistribution and clearance study. Here we choose only two months aged male mice as the animal model. The as-prepared N-doped CQDs (final dose ~5 mg/kg) were injected intraperitoneally into the mice (27 mice). The mice were sacrificed (n=3/day) at 1, 2, 3, 4, 5, 6 and 7 days of post injection. The presence/absence of N-doped CQDs in major organs and tissues were determined by fluorescence microscopy to monitor their fluorescence intensity level. The biodistribution data were presented in Figure 5a. 1st 48 hours of the post injection the liver was the dominant organ for N-doped CQDs accumulation, followed by the kidney. Lung, muscle and urinary sac showed relatively low fluorescence intensity means low concentration of N-doped C-QDs accumulation. But 6 days of post injection no accumulation shown in any studied organs and tissues. Kidney is the main organ for foreign particle clearance from the blood. And we also observed a drastic

decrease of fluorescence intensity in blood and excretory materials as N-doped CQDs were completely cleared through urine and faeces within 6 days of post injection (Figure 5b, c, d). In Supporting Information Figure S8 exhibited the true fluorescence images of blood, faeces and urine.

Conclusions

In summary high quantum yielding (ca 74.16%) N-doped CQDs were synthesized and their chemical structure, fluorescence mechanism, toxicity, bioimaging applications, bio distributions and clearances were studied successfully. N-doped CQDs shown very strong ionic strength and stability under long range pH 2-13 which will be very important for pharmaceutical applications. Quicker clearance efficiency without accumulation in organs and tissues were also studied. Where other metal nanomaterials causing organ damage due to their long term accumulation (90 days or more) in organs and tissues.[47-51] Finally we can conclude that our durable N-doped CQDs are harmless and nontoxic in biomedical and bioimaging fields. Also, it could potentially be used in printing industry as N-doped CQDs were successfully applied as printing inks for multicolour patterns.

Acknowledgment. Tapas K. Mandal and Nragish Parvin would like to thank SERB, DST, (Project File no- SR/FT/LS-76/2012) and DBT Government of India for providing financial support respectively. Also thanks to “Chinese Academy of Science postdoctoral and Visiting scholar for developing country programme” for financial support.

References

1. Y. Wang, Z. Li, J. Wang, J. Li, Y. Lin., *Trends Biotechnol.* 2011, **29**, 205-212.
2. N. Parvin, T.K. Mandal, P. Roy, *J Nanosci Nanotechno*l. 2013, **13** (10), 6499-505.
3. T.K. Mandal, N. Parvin, *J Biomed Nanotechnol*. 2011, **7**(6), 846-8.
4. W. Nakanishi, K. Minami, L. K. Shrestha, Q. Ji, J. P. Hill, K. Ariga, *Nano Today*. 2014, **9**, 378-394.

5. M. Aramesh, W. Tong, K. Fox,A. Turnley,D. H. Seo,S. Prawer and K. K. Ostrikov, *Materials.*2015,***8*(8),** 4992-5006.
6. Z. Fan, S. Li, F. Yuan and L. Fan. *RSC Adv*. 2015, **5**, 19773–19789.
7. K. Minami, Y. Kasuya, T. Yamazaki, Q. Ji, W. Nakanishi, J. P. Hill, H. Sakai, and K. Ariga. *Adv. Mater.* 2015, ***27*,** 4020–4026.
8. S. Mazumder, R. Dey, M.K. Mitra, S. Mukherjee, G.C. Das, *J. Nanomater.* 2009, 1-17.
9. K.J. Lee, P.D. Nallathamby, L.M. Browning, C.J. Osgood, X.H.N. Xu, *Acs Nano.* 2007, **1**, 133–143.
10. J.K. Jaiswal, H. Mattoussi, J.M. Mauro, S.M. Simon, *Nat. Biotechnol. 2003,* **21**, 47–51.
11. Y.Q. Zhang, D.K. Ma*, Y.* Zhuang*,* X. Zhang*, W. Chen, L.L. Hong*, Q.X. Yan, K.Yu, S.M. Huang, *J. Mater. Chem*.2012, **22**, 16714-16718.
12. A.M. Derfus, W.C.W. Chan, S.N. Bhatia, *Nano Lett.* 2004, **4**, 11-18.
13. D. Bera, L. Qian, T.K. Tseng, P.H. Holloway, *A Review. Materials.*2010, **3**, 2260-2345.
14. C.J. Liu, P.Zhang, X.Y. Zhai, F. Tian, W.C. Li, J.H. Yang, Y. Liu, H.B. Wang, W. Wang, W.G. *Liu*, *Biomaterials*. 2012, **33**, 3604-3613.
15. J.G. Zhou, C. Booker, R.Y. Li, X.T. Zhou, T.K. Sham, X.L. Sun, Z.F. Ding, *J. Am. Chem. Soc*. 2007,**129**, 744-745.
16. S.N. Baker, G.A. Baker, *Angew. Chem. Int. Ed.* 2010, **49**, 6726-6744.
17. C. Ding, A. Zhu, Y Tian, *Acc.Chem. Res.* 2014*,* **47**, 20-30.
18. S. Zhu, Q. Meng, L. Wang, J. Zhang, Y. Song, H. Jin, K. Zhang, H. Sun, H. Wang, B. Yang, *Angew. Chem. Int. Ed*. 2013, **52**, 3953-3957.
19. X. Feng, Y. Jiang, J. Zhao, M. Miao, S. Cao, J. Fang and L. Shi, RSC Adv., 2015, **5**, 31250–31254
20. Y. Dong, R. Wang, G. Li, C. Chen, Y. Chi and G. Chen, Anal. Chem., 2012, **84**, 6220.
21. H. Ding, J.S. Wei, H.M. Xiong, *Nanoscale,* 2014, **6,** 13817.

22. J. Wang, C.F. Wang, S. Chen,. *Angew. Chem. Int. Ed.* 2012, **51**, 9297-9301.

23. G.Jiang, T. Jiang, H. Zhou, J. Yao, X. Kong, *RSC Adv.* 2015, **5**, 9064-9068.

24. H.S. Choi, W. Liu, P. Misra, E. Tanaka, J.P. Zimmer, B.I. Ipe, M.G. Bawendi, J.V. Frangioni, *Nat Biotech*. 2007, **25**, 1165-70.

25. G. Sonavane, K. Tomoda, K. Makino, *Colloids Surf B Biointerfaces*. 2008, **66**, 274-80.

26. N. Farrell, 1989, **11**. Boston, MA: Kluwer Academic Publishing.

27. D.M. Herold, I.J. Das,C.C. Stobbe, R.V. Iyer, J.D. Chapman, *Int J Radiat Biol*. 2000, **76**, 1357-64.

28. S.J. Bakri, J.S. Pulido,P. Mukherjee, R.J. Marler, D. Mukhopadhyay, *Retina*. 2008, **28**,147-9.

29. L.W. Zhang, W.W. Yu, V.L. Colvin, N.A. Monteiro-Riviere, *Toxicol Appl Pharmacol*. 2008, **228**, 200-11.

30. S. Sahu, B. Behera, T.K. Maiti, S. Mohapatra, *Chem. Commun.* 2012, **48**, 8835-8837.

31. C. Mattevi, G. Eda, S. Agnoli, S. Miller, K.A. Mkhoyan, O. Celik, D. Mastrogiovanni, G. Granozzi, E. Garfunkel, M. Chhowalla, *Adv. Funct. Mater*. 2009, **19**, 2577.

32. M. Vedamalai, A.P. Periasamy, C.W. Wang, Y.T. Tseng, L.C. Ho, C. Shih, H.T. Chang, *Nanoscale*. 2014, **6**, 13119.

33. Z. Qian, J. Ma, X. Shan, H. Feng, L. Shao, J. Chen, *Chemistry*. 2014, **17**;20(8):2254-63.

34. W. Wang, Y.C. Lu, H. Huang, J.J. Feng, J.R. Chen, A.J. Wang, Analyst. *2014,* **139**, 1692–1696.

35. R. Zhang, W. Chen, *Biosen. Bioelectron*. 2014, **55**, 83–90.

36. R. Liu, D. Wu, S. Liu, K. Koynov, W. Knoll, Q. Li, Angew. Chem. 2009, **121**, 4668 - 4671; *Angew. Chem. Int. Ed*. 2009, **48**, 4598 – 4601.

37. M.J. Krysmann, A. Kelarakis, P. Dallas, E.P. Giannelis, *J. Am. Chem. Soc*. 2012, **134,** 747-750.

38. H. Liu, T. Ye, C. Mao, C. Angew. Chem. 2007, **119**, 6593 – 6595; *Angew. Chem. Int. Ed.* 2007, **46**, 6473- 6475.

39. X. Zhai, P. Zhang, C. Liu, T. Bai, W. Li, L. Dai,W. Liu, *Chem. Commun*. 2012, **48**, 7955-7957.

40. D. Pan, J. Zhang, Z. Li, C. Wu, X. Yan, M. Wu, *Chem. Commun*. 2010, **46**, 3681-3683.

41. J. Shang, L. Ma, J. Li, W. Ai, T. Yu, G.G. Gurzadyan, *Sci. Rep*. *2012,* **2**, 792.

42. D. Wang, X. Wang, Y. Guo, W. Liu, W. Qin, *RSC Adv*. 2014, **4**, 51658.

43. A. Mewada, S. Pandey, M. Thakur, D. Jadhav, M. Sharon, *J. Mater. Chem. B*. 2014, **2**, 698.

44. S.L. Hu, K.Y. Niu, J. Sun, J. Yang, N.Q. Zhao, X.W. Du, X.W. *J. Mater. Chem*. 2009, **19**, 484.

45. S. Qu, X. Wang, Q. Lu, X. Liu, L. Wang, Angew. Chem. 2012, **124**, 12381-12384; *Angew. Chem. Int. Ed*. 2012, **51**, 12215-12218.

46. Y. Dong, J. Shao, C. Chen, H. Li, R. Wang, Y. Chi, X. Lin, G. Chen, *Carbon*. 2012, **50**, 4738-4743.

47. X.D. Zhang, Z. Luo, J. Chen, H. Wang, S.S. Song, X. Shen, W. Long, Y.M. Sun, S. Fan, K. Zheng, D.T. Leong, J. Xie, J. *small*. 2015, *11,* No. **14**, 1683-1690.

48. X.D. Zhang, D. Wu, X. Shen, P.X. Liu, F.Y. Fan, S. Fan, *J. Biomaterials*. 2012, **33**, 4628-4638.

49. M. Setyawati, C. Tay, S. Chia, S. Goh, W. Fang, M. Neo, H. Chong, S.Tan, S. Loo, K. Ng, J. Xie, C. N. Ong, N.S. Tan, N. S.; D.T. Leong, *Nat. Comm*. 2013, **4**, 1673.

50. X.D. Zhang, D. Wu, X. Shen, J. Chen, Y.M. Sun, P.X. Liu, X.J. Liang, *Biomaterials*. 2012, **33**, 6408.

51. X.D. Zhang, D. Wu, X. Shen, P.X. Liu, N. Yang, B. Zhao, H. Zhang, Y.M. Sun, L.A. Zhang, F.Y. Fan, Int. *J. Nanomed*. 2011, **6**, 2071.

FIGURES AND FIGURES CAPTIONS (1 to 4)

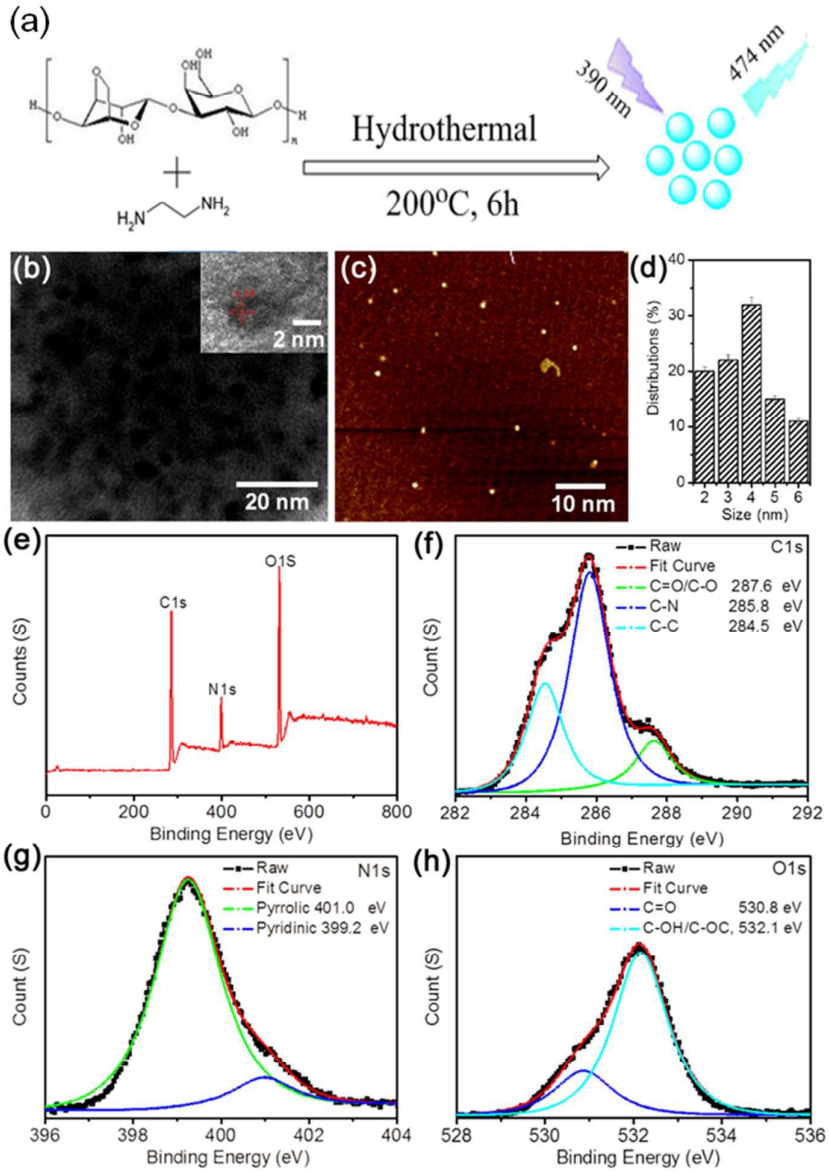

Fig 1.(a) Schematic illustration of N-CQDs formation by hydrothermal treatment; (b) low and high magnified (inset)TEM images of N-CQDs; (c) AFM images of N-CQDS; (d) particle size distribution of N-CQDs; (e) XPS spectrum of N-CQDs. High-resolution XPS spectra of C1s (f), N1s (g) and O1s(h).

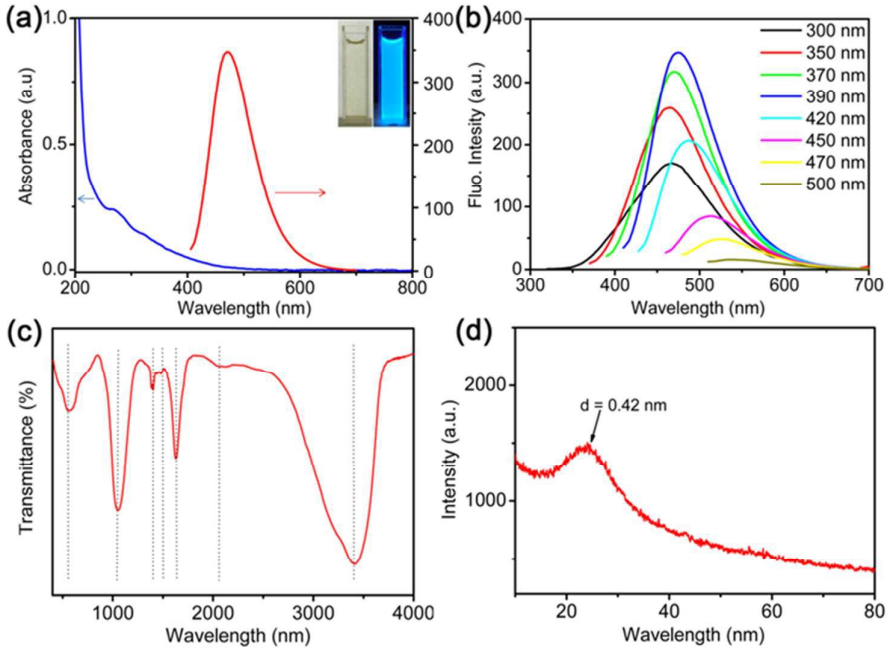

Fig 2. a) UV/Vis absorption (blue line), fluorescence emission (red line) of N-CQDs Where excitation 390nm emission 494 nm and insets show photographs of N-CQDs in aquatic media under white and hand held UV lamp, (b) excitation depended emission spectra of aqueous N-CQDs solution ($0.01 mgmL^{-1}$). (c) FTIR Spectrum of N-CQDs and (d) XRD pattern of N-CQDs.

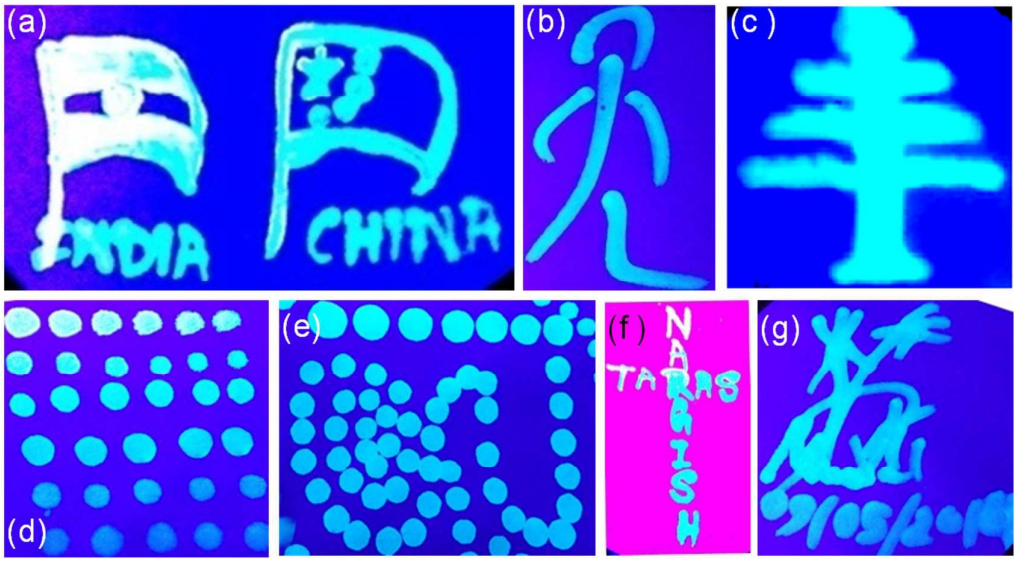

Fig 3. Printed patterns obtained by N-CQDs ink (illuminated by a portable UV lamp). (a,b,c) Different concentrated N-CQDs ink used letter and graphic pattern. (d,e) Different concentrated N-CQDs ink give different intensity images pattern. (f) Different concentrated N-CQDs ink to obtain different color letters. And (g) image of print after 1.6 years exposed to laboratory ambient environment.

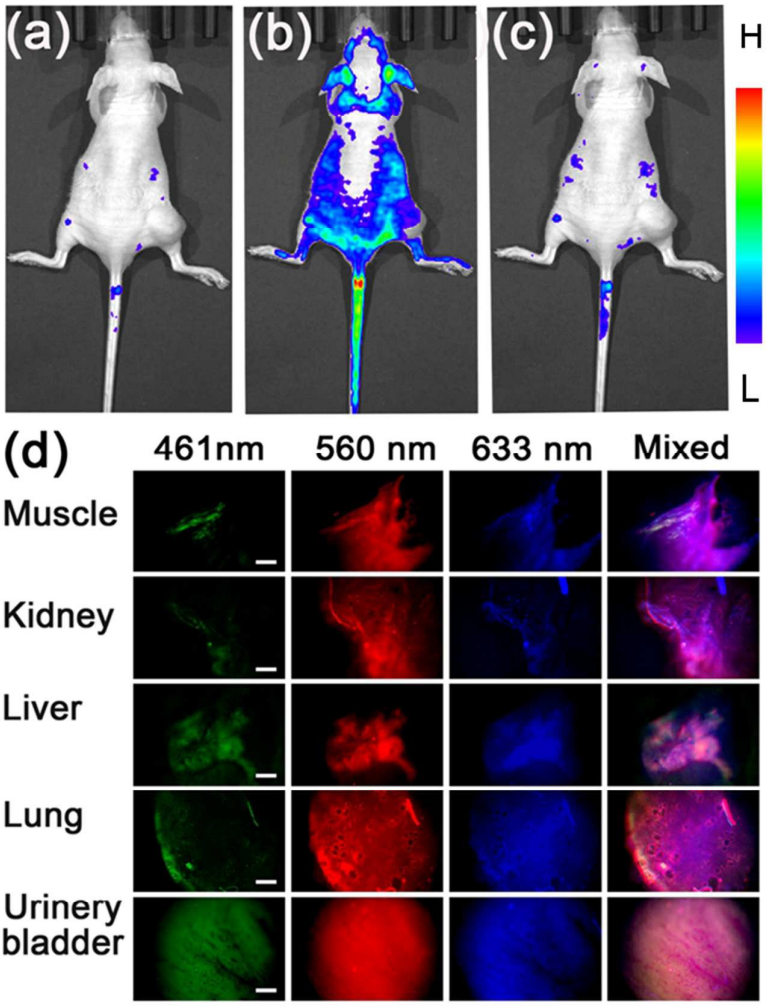

Fig 4. Whole body fluorescence images of nude mice in different time of injection (a) pre injection, (b) 12 hours after Post injection, (c) 24 hours after post injection. (d) Fluorescence microscopy images of different organs and tissues under different band pass filters. Where organs and tissues collected from 1 hour of post injected mice. Scale bar is 50 µm.

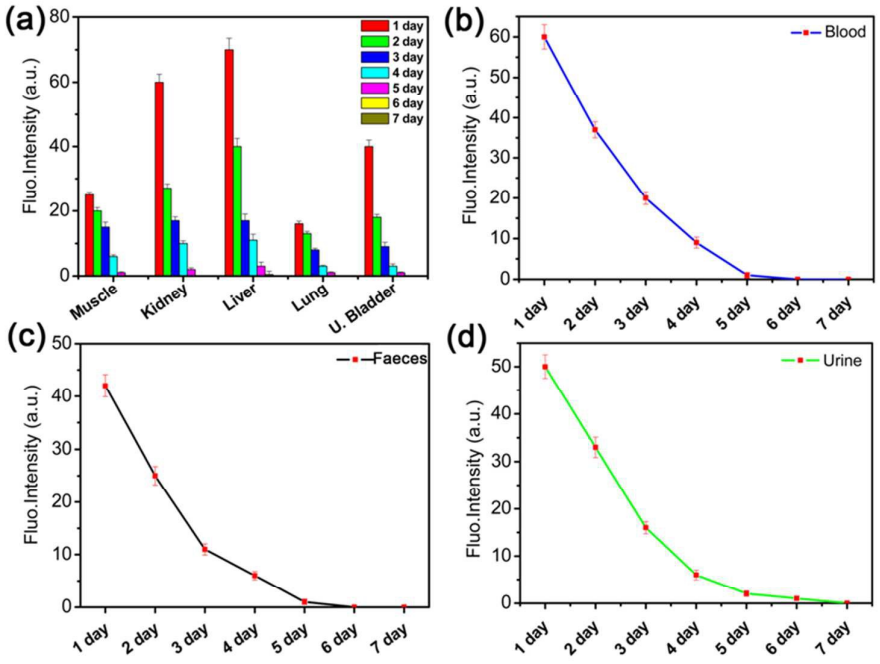

Fig 5. (a) Distributions of N-CQDs probe in different organs and tissues of nude mice determined at 1 to 7 days of postinjection. Postinjection clearance profile of N-CQDs in different time from 1 to 7 days through (b) blood; (c) faeces and (d) urine.

Graphical Abstract